Progress In Electromagnetics Research C, Vol. 83, 45–56, 2018

Surface Plasmon Effects and Resonance State on Square Lattice of Metallic Photonic Crystals and Defect Mode in H Polarization

Khee Lam Low[1, *], Mohd Zubir Mat Jafri[2], Sohail A. Khan[2], and Donald G. S. Chuah[2]

Abstract—The surface plasmon effect in metallic photonic crystals has been investigated. Band structure graph is the only graph that can be used to explain the characteristics of photonic crystals. In this work, band structure graphs have been used to describe these characteristics, which include the surface plasmon effect of photonic crystals. Recently, band structure graphs for frequency-dependent materials have been analyzed by several researchers. The surface plasmon effect has been found for these materials. This article reports the effect of surface plasmons which cause resonance state in the metallic photonic crystals when the relative permittivity is changed from band structure graphs. The numerical results from the commercial software show the magnetic field distribution of waves on the normal photonic crystals, and defect mode is added for each frequency.

1. INTRODUCTION

Photonic crystals have been extensively developed since the prediction and investigation of Yablonovitch [1] and John [2]. This active research has been extended to metallic photonic crystals, and more characteristics of photonic crystals are expected to be discovered compared with the conventional dielectric-dielectric photonic crystals [3–23]. It is well known that electromagnetic waves with frequencies lower than the plasma frequency of metals cannot propagate through a bulk metal. However, it is possible for electromagnetic waves to be guided below the plasma frequency and attributed to the surface plasmon effect if an array of dielectric components is embedded in the bulk metals [24].

Kuzmiak et al. studied the dispersion relation of photonic crystals containing metallic components in two dimensions (2D) using the plane wave expansion method and Drude model [10–12]. Low et al. continued their calculation by studying metallic photonic crystals using the modified plane wave expansion method with the Drude model with different dielectric rods in the E polarization mode [24–26]. Several characteristics were observed in the dispersion relation graphs, such as flat bands occurring at some of the frequencies, a group velocity anomaly in the band edges, and an effective plasma frequency in the E polarization mode. The H polarization mode has also been extensively studied by several scientists [8, 10, 11]. Kuzmiak and Maradudin [10, 11] calculated band structure graphs for frequency-dependent materials in a vacuum background using the plane wave expansion method. They also included the damping frequency of the metallic component in their calculation. However unfortunately, their calculation was limited to only air or vacuum backgrounds. Their calculation was generalized by Low et al. [27]. Then, Low et al. [24, 26] continued the development of the band structure equation for photonic crystals in metals. The surface plasmon effect was detected in the band structure graphs in this investigation. Then, there is an increase of interest of the surface plasmon polariton based sensors [28–31]. The performance of the sensors increases with the amount of field confinement. In our study, magnetic field distribution diagram is plotted, and wave confinement can be seen clearly.

Received 16 January 2018, Accepted 24 March 2018, Scheduled 8 April 2018
* Corresponding author: Khee Lam Low (kheelam.low@kdupg.edu.my).
[1] KDU Penang University College, Penang, Malaysia. [2] Universiti Sains Malaysia, Penang, Malaysia.

In the first section of this paper, a plane wave expansion method for metallic photonic crystals with different dielectric rods in H polarization mode is used. Even though this method faced convergence problem [32], it is still the fastest way to find the band structure graph. Some results using PWE have been published [8, 11, 14, 33, 34], but they have not included any extensive discussions of the surface plasmon effect when relative permittivity is changed. The surface plasmon effect is very obvious in band structure graphs at first glance [24]. So, in this paper, we investigate the surface plasmon effect when the relative permittivity of rods is changed in the metallic photonic crystals in H polarization. Because the band structure graph presents only the energy change in the metallic photonic crystals, we needed a commercial package to observe the magnetic field pattern that localized in the dielectric rods. The investigation also only focuses on frequencies lower than plasma frequency in which metal is forbidden to waves. The occurrence of magnetic field distributions at each flat band has been investigated by using the OptiFDTD software.

Then, in the second section of this paper, magnetic field pattern of the defect mode of the metallic photonic crystals is investigated. The objective of the study is to observe the resonance state of dielectric rods caused by surface plasmon at a frequency lower than the metal plasma frequency. This resonance state has been reported by several investigators [35, 36]. The uniqueness of this resonance state can cause waves to propagate even though at frequencies which are not transparent to waves. The study is performed by using time domain package which is OptiFDTD, and magnetic field distribution graph is observed and discussed.

2. PHOTONIC BAND STRUCTURE GRAPH OF METALLIC PHOTONIC CRYSTALS WITH DIELECTRIC RODS

We sketch a cross-section view of the photonic crystals in Figure 1.

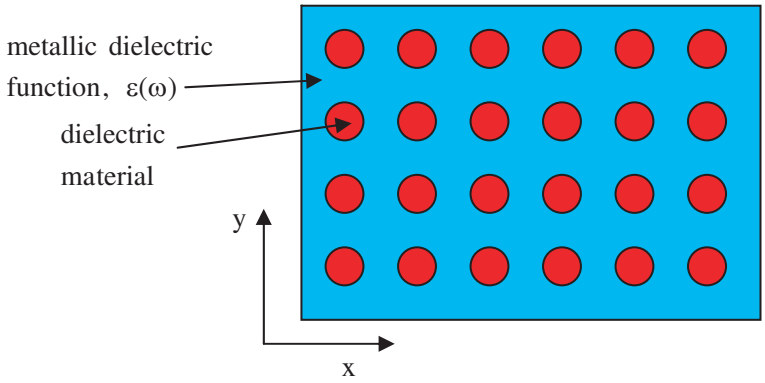

Figure 1. Illustration of the metallic photonic crystals arrangement (square lattice).

The band structure graph is derived for H polarization which has only magnetic field in the wave propagation direction for metallic photonic crystals with dielectric rods [37, 38] in Equation (1):

$$\varepsilon_0\mu^2 A(k|G) - \mu \left[\begin{array}{l} \left(\varepsilon_0 + \varepsilon_0 \dfrac{c^2}{\omega_p^2} |k+G|^2\right) A(k|G) \\ + (1-\varepsilon_0) \dfrac{c^2}{\omega_p^2} \displaystyle\sum_{G'} (k+G)\cdot(k+G') 2f \frac{J_1(|G-G'|R)}{|G-G'|R} A(k|G') \end{array} \right]$$
$$+ \frac{c^2}{\omega_p^2} \sum_{G'} (k+G)\cdot(k+G') 2f \frac{J_1(|G-G'|R)}{|G-G'|R} A(k|G') = 0 \quad (1)$$

where $\mu = \omega/c$, ε_0 is the relative permittivity, k the wave vector, G the reciprocal lattice, J_1 the first Bessel function, R the radius of the rods, ω_p the plasma frequency of the metals, c the speed of light,

and ω the eigenfrequency. Equation (1) represents a generalized eigenvalue problem. A linearization technique is used. An equation in the following form is obtained:

$$\mu^2 \overleftrightarrow{J} - \mu \overleftrightarrow{K} + \overleftrightarrow{L} = 0 \tag{2}$$

where the elements $\overleftrightarrow{J}$,$\overleftrightarrow{K}$, and $\overleftrightarrow{L}$ of $NG \times NG$ matrices are given as

$$\overleftrightarrow{J} = \varepsilon_\circ \tag{3}$$

$$\overleftrightarrow{K} = \left[\left(\varepsilon_\circ + \varepsilon_\circ \frac{c^2}{\omega_p^2} |k+G|^2\right) A(k|G) + (1-\varepsilon_\circ)\frac{c^2}{\omega_p^2} \sum_{G'} (k+G)\cdot(k+G') 2f \frac{J_1(|G-G'|R)}{|G-G'|R} A(k|G')\right] \tag{4}$$

$$\overleftrightarrow{L} = \frac{c^2}{\omega_p^2} \sum_{G'} (k+G)\cdot(k+G') 2f \frac{J_1(|G-G'|R)}{|G-G'|R} A(k|G') \tag{5}$$

Equation (2) is a second-order eigenvalue problem, which can be represented by the following matrix form:

$$\overleftrightarrow{M} = \begin{pmatrix} 0 & I\overleftrightarrow{J} \\ \overleftrightarrow{K} & \overleftrightarrow{L} \end{pmatrix} \tag{6}$$

The complete solution of Equation (6) is obtained by solving the eigenvalues of $\overleftrightarrow{M}$ using the diagonalization of this non-Hermitian matrix.

3. RESULT AND DISCUSSION

3.1. Periodic Structure

In this article, four examples of different materials with the same filling fraction $f = 0.5$ are used as cylindrical rods in a copper medium. The plasma frequency of copper is $\omega_p = 1914$ THz. The band structure graphs are plotted along $M(\frac{\pi}{a}, \frac{\pi}{a})$-$\Gamma(0,0)$-$X(\frac{\pi}{a}, 0)$ in the first irreducible Brillouin zone. The magnetic field distribution graphs are plotted at $k = 0$ with their respective frequencies. The dimensions of photonic crystals are in micrometers.

From the Drude Model, there should be no wave activities inside the metallic structure below the plasma frequency. The model will become free electron gas model. Then, metals should reflect light in the visible region and be transparent to light at high frequencies [39]. However from the previous investigation [24], wave activities below the plasma frequency are detected. This is because the structure of metallic photonic crystals structure exhibits a very special characteristic, which is the surface plasmon effect. The band structure graph of copper photonic crystals with air rods is plotted in Figure 2(a). The band structure graph has a lot of flat bands. To confirm the effect of surface plasmons, OptiFDTD software is used to investigate the magnetic field distribution of the photonic crystals at $k = 0$ at each frequency. Figure 2(b) shows the magnetic field distribution with the frequency at 1280 THz ($\frac{\omega a}{2\pi c} = 0.68$). Obviously, surface plasmon effect is detected at this frequency, and we find that some of the waves are inside the air rods. Then, the frequency used in the magnetic field distribution graph is lowered to 537 THz ($\frac{\omega a}{2\pi c} = 0.28$), and the result is shown in Figure 2(c). The wave is only on the surface of the air rods, which is the surface plasmon, and no wave is inside the rods. Then the frequency is further lowered to 185 THz ($\frac{\omega a}{2\pi c} = 0.098$), and the magnetic field distribution graph of this frequency is shown in Figure 2(d). There is a complete wave localized (peak to valley wave) across the air rods. The frequency range shows that the wave is near the surface of the rods. This agrees very well with the band structure graph. Flat bands in all the mentioned frequency points in the band structure graph are evidence of the surface plasmon effect [40]. However, the flat bands vanish when $\frac{\omega a}{2\pi c} \geq 1$. This corresponds to the fundamental metallic characteristic where the wave is able to propagate in a metal when the frequency is larger than the plasmon frequency. In this region, the metal behaves as free electron model, and metal is transparent to wave. The magnetic field distribution graph of photonic crystals at $\frac{\omega a}{2\pi c} = 1.2$ (2255 THz) is plotted in Figure 2(e). The wave propagates randomly across the air rods. So, it is obvious that the wave is distributed around the rods at frequencies below $\frac{\omega a}{2\pi c} = 1.2$.

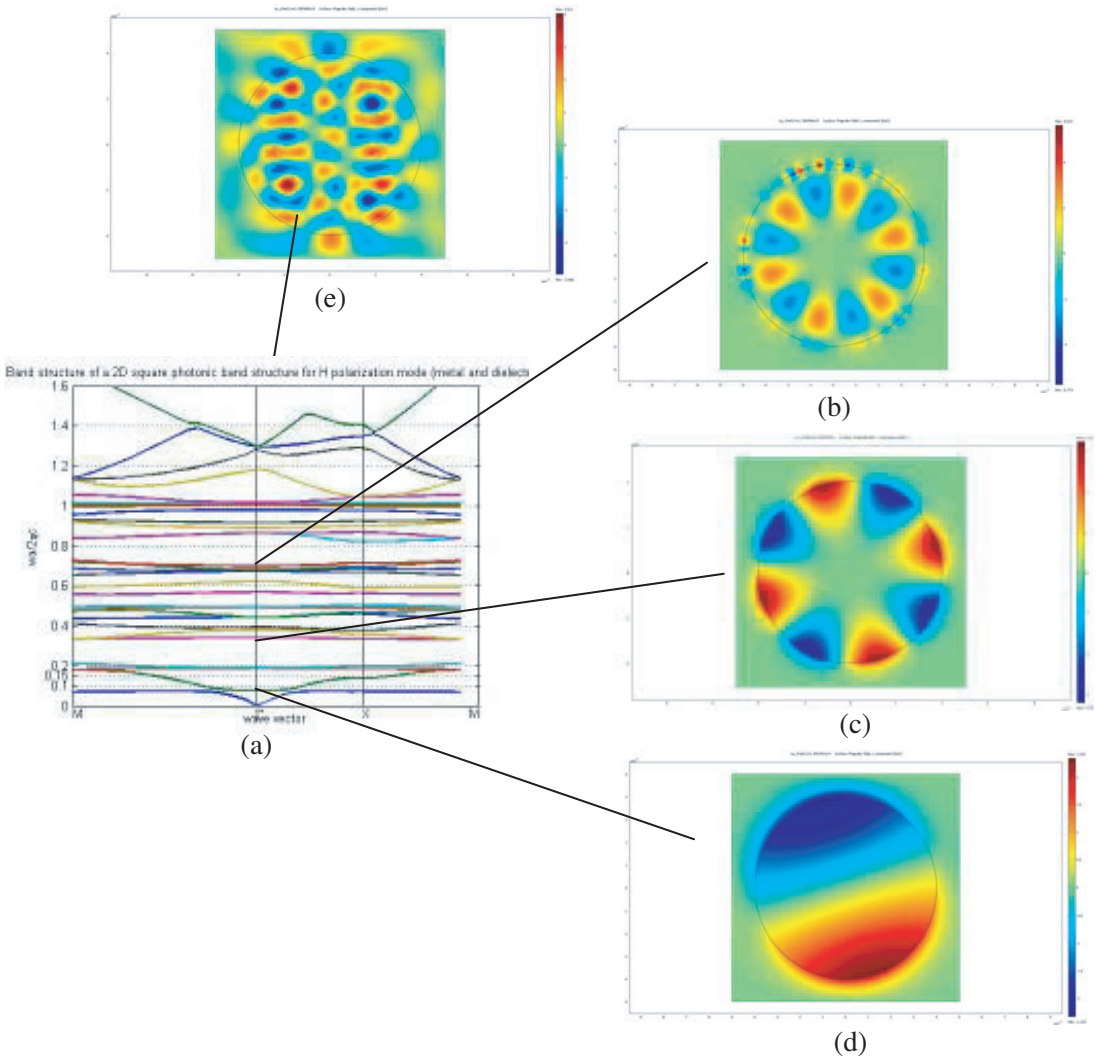

Figure 2. (a) Band structure graph of air rods with filling fraction $f = 0.5$ in the copper medium in H polarization mode. Magnetic field distribution at frequency (b) 1280 THz, (c) 537 THz, (d) 185 THz, (e) 2255 THz.

All the waves below this frequency are surface plasmon waves. This is described very well in the band structure graph.

Equation (1) is utilized to plot the band structure graph of a Teflon ($\varepsilon_\circ = 2$) rod in the copper medium as shown in Figure 3(a). The band structure graph is very similar to the band structure graph of Figure 2(a). It has several flat bands below the normalized frequency, $\frac{\omega a}{2\pi c} = 0.8$, and the frequency is lower than that of the previous structure. The flat band at the edge of the band gaps is created due to the highly localized resonances within the dielectric rods [35]. A band gap appearing in the frequency range $0.8 \leq \omega a/2\pi c \leq 1$ shows that this structure is a typical photonic crystal structure. Further, the magnetic field distributions at frequencies 1279 THz, 728 THz, and 138 THz are shown in Figures 3(b), 2(c), and 2(d), respectively. In Figure 3(b), the wave is localized in the Teflon rods and found on the surface of the rods. Figure 3(c) shows the same characteristic with a longer wavelength. Figure 3(d) shows that a complete wave is localized in the Teflon rods.

Then the dielectric constant of rods is increased to $\varepsilon_\circ = 4.9$ which is FR-4. FR-4 is an insulator which is very common in the electronics industry. The band structure graph is plotted in Figure 4(a). It is obvious that flat bands are fewer; they are situated below the normalized frequency $\frac{\omega a}{2\pi c} = 0.6$. The magnetic field distributions of the flat bands at $\frac{\omega a}{2\pi c} = 0.34$ (646 THz) and $\frac{\omega a}{2\pi c} = 0.075$ (142 THz)

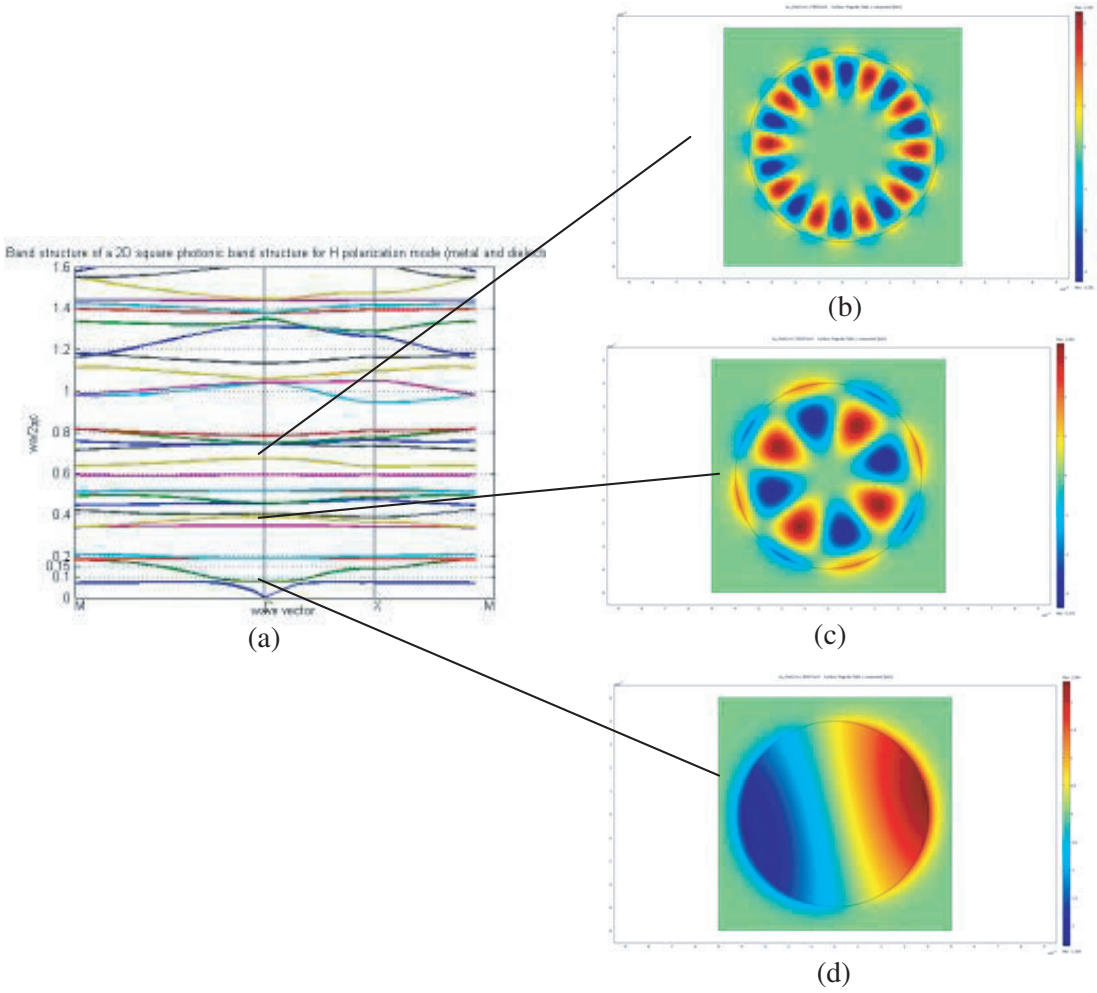

Figure 3. (a) Band structure graph of Teflon rods with filling fraction $f = 0.5$ in the copper medium in H polarization mode. Magnetic field distribution at frequencies (b) 1279 THz, (c) 728 THz, and (d) 138 THz.

are plotted in Figures 4(c) and 4(d), respectively. In Figure 4(c), the wave is localized not only on the surface of the FR-4 rods but also inside the FR-4 rods. The wave is in quadrupole mode. In Figure 4(d), the waveform is different from the waveform of air and Teflon rods. In the air and Teflon rods, there is a complete wave propagating across the rods. However in the FR-4 rods, the waveform is separated into two complete waves, localized around the surface of the rods. The wave is now in dipole mode. The phenomenon that appears in Figure 2(e) is found in Figure 4(b). The wave is propagating irregularly. However, the frequency of Figure 4(b) is lower than that in Figure 2(e). It shows that the wave is propagating in the FR-4 rods at the lower frequency.

The dielectric constant of the rods is further increased to 12.96 in the case of gallium arsenide (GaAs). The band structure graph is plotted in Figure 5(a). The flat bands are less frequent than the three materials investigated earlier. This means that the effect of surface plasmons is reduced. The magnetic field distribution of $\frac{\omega a}{2\pi c} = 0.093$ (176 THz) is shown in Figure 5(d). The waves are localized near the surface of the GaAs rods. However, when the frequency is increased to $\frac{\omega a}{2\pi c} = 0.39$ (743 THz), the waves are propagating out from the center of the GaAs rods. The waves are in dipole mode. The magnetic field distribution graph is shown in Figure 5(c). It no longer shows a surface plasmon effect. Then, the frequency is further increased to $\frac{\omega a}{2\pi c} = 0.80$ (1499 THz); the waves are oscillating around the GaAs rods. The waves are in odd number oscillating mode.

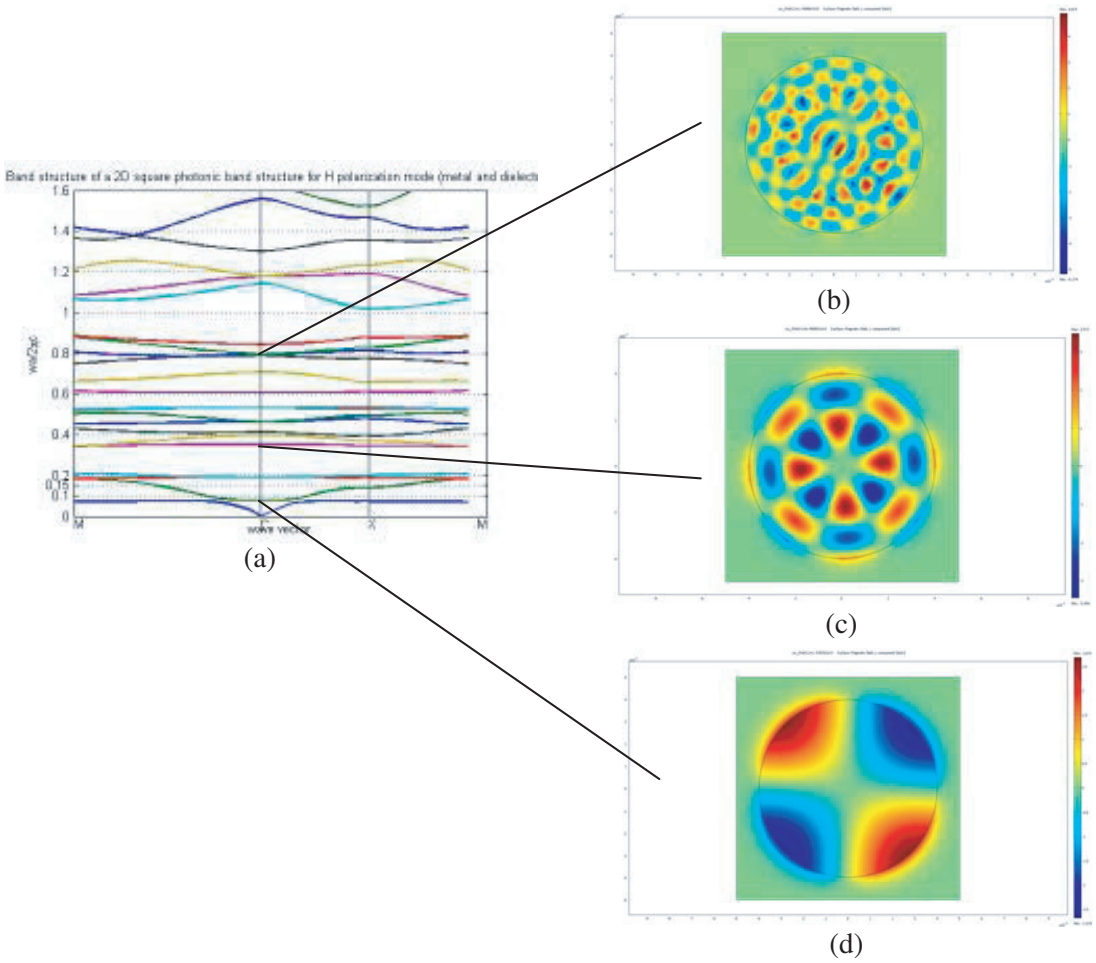

Figure 4. (a) Band structure graph of FR-4 rods with filling fraction $f = 0.5$ in the copper medium in H polarization mode. Magnetic field distribution at frequencies (b) 1491 THz, (c) 646 THz, and (d) 142 THz.

The surface plasmon effect is reduced from vacuum to GaAs. The flat bands that represent the surface plasmon effect are less frequent when the relative permittivity of rods is increased. So, when a high relative permittivity material is coupled with metals, the surface plasmon effect is not obvious. The structure will act as an ordinary photonic crystal, free of flat bands, while the relative permittivity of rods is increased. From the magnetic field distribution figure, the waves are localized inside the dielectric rods, especially for frequencies lower than the plasma frequency for all materials. The motion of the solid state plasma, whose characteristic is the plasma frequency in metals, is confined to the interior of the dielectric rods. So, the characteristic that an electromagnetic wave cannot penetrate metals can be overcome by insertion of an array of dielectric rods in metals.

3.2. Defect Mode

The magnetic field distribution diagrams show that the field is oscillating and localized inside the dielectric materials causing the surface plasmons effect trapped inside the dielectric rods. Figure 3 to Figure 5 show different modes of the surface plasmons inside the dielectric rods. All these happen below the plasma frequency in which metal is forbidden to wave [39]. So, the investigation continues by using 9 layers of defect mode by removing one rod at the center as shown in Figure 6. The simulation is done by using OptiFDTD and places a point source at the center of the defect structure. This method is different from that by Qiu and He [41] which used a plane wave. However, the results are the same.

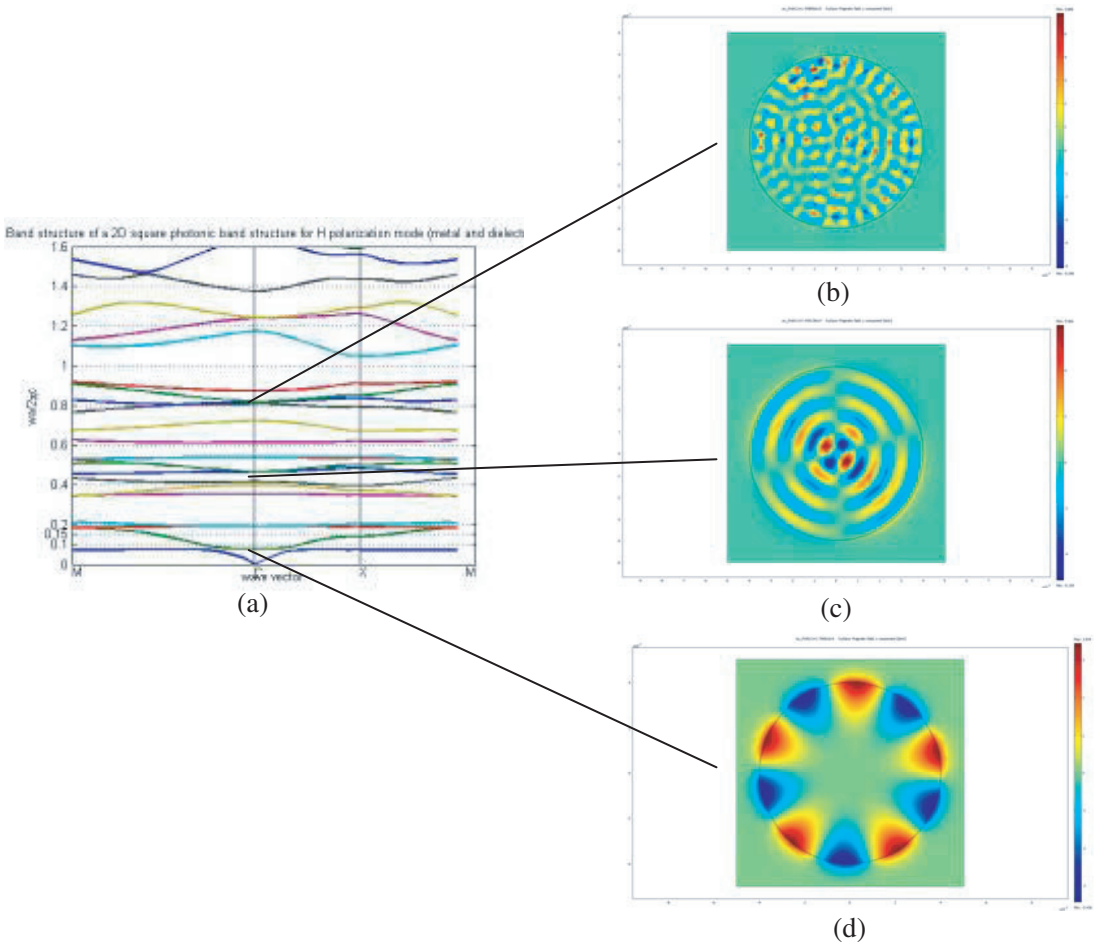

Figure 5. Band structure graph for GaAs rods with filling fraction $f = 0.5$ in the copper medium in H polarization. Magnetic field distribution at frequencies (b) 1499 THz, (c) 743 THz, and (d) 176 THz.

The main focus of this study is to understand the effect of whether the dielectric rods will cause the resonance state and help the wave to propagate in metal. The structure is covered by a perfect match layer so that all the wave will be absorbed in the boundaries.

The frequency used is 1491 THz, and the dielectric rods has a dielectric constant of 4.9. The magnetic field distribution diagram is obtained in Figure 7. It can be seen clearly that the wave is propagating out in the direction of Γ, X and M. The wave is trapped or localized inside the dielectric rods. This unique oscillating behavior causes resonance effect, and wave is now propagating inside the metal even lower than the plasma frequency.

To simulate 9 layers of dielectric rods requires more time than fewer layers, and the results are the same as the structure which is periodic in all directions. So, the study size is reduced to 3 layers as shown in Figure 8. The simulation study is focused on dielectric rods = 4.9 and dielectric rods 12.96. The selection of frequencies is from Figure 3 to Figure 5. Figure 9 shows the near-field magnetic field distribution 646 THz for dielectric rods = 4.9. It can be seen clearly that the wave is in resonance state at all the nearby dielectric rods, and this resonance state causes the wave to propagate at a lower frequency.

Then, the dielectric constant is increased to 12.96. Figure 10 shows the near-field magnetic field distribution at 1499 THz, and the wave is in dipole mode. Figure 11 shows the near-field magnetic field distribution at 743 THz, and the wave is in two modes: dipole and hexapole modes. Figure 10 and Figure 11 show that no matter at higher or lower frequency, the wave is still able to be resonant inside the dielectric rods. However, compared to lower dielectric constant, the wave is more confined.

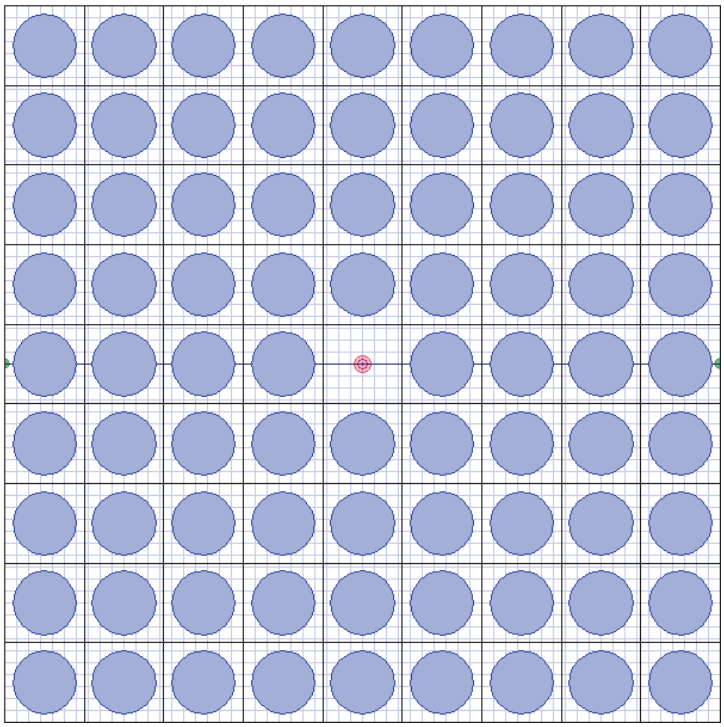

Figure 6. Schematic diagram of the defect mode with 9 layers of dielectric rods.

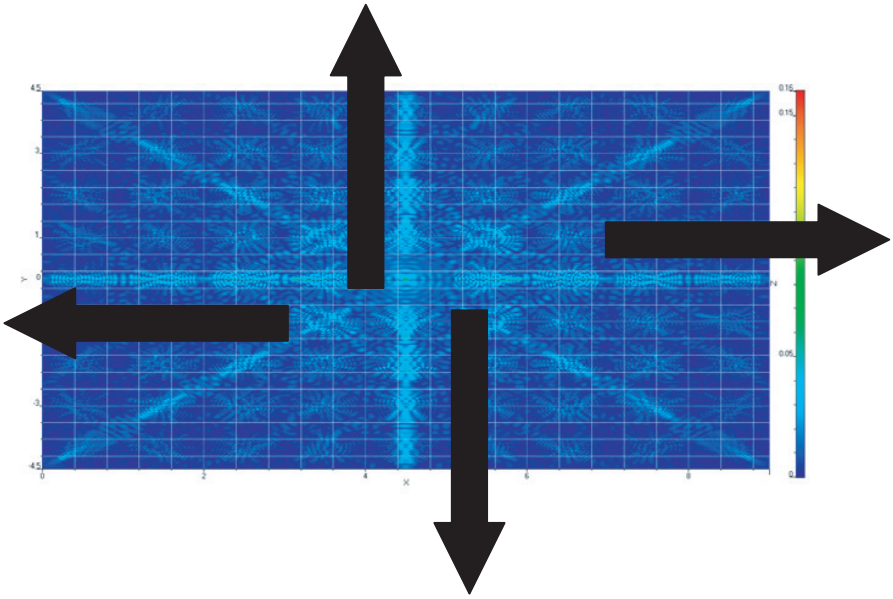

Figure 7. Magnetic field distribution of frequency = 1491 THz and dielectric rods = 4.9. The 4 black arrows showed the direction of the propagation of the wave.

The surface plasmon effect of the metal causing the wave can be localized in the dielectric rods which is the resonance state in the dielectric rods. This effect is the result due to strong field confinement in the defect mode [36]. Then this causes the wave to propagate through the metal even not more than the plasma frequency.

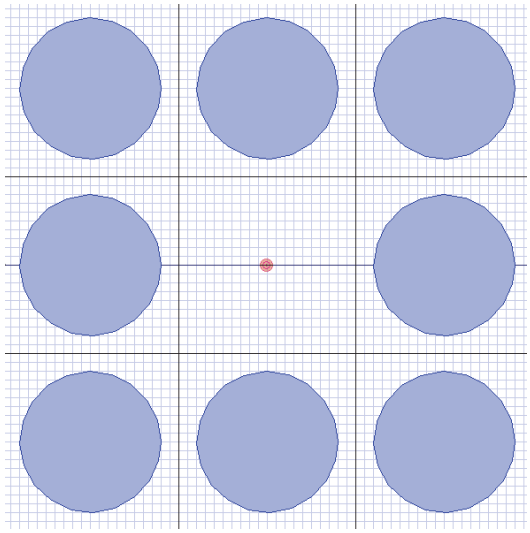

Figure 8. Schematic diagram of the defect mode of the 3 layers of dielectric rods.

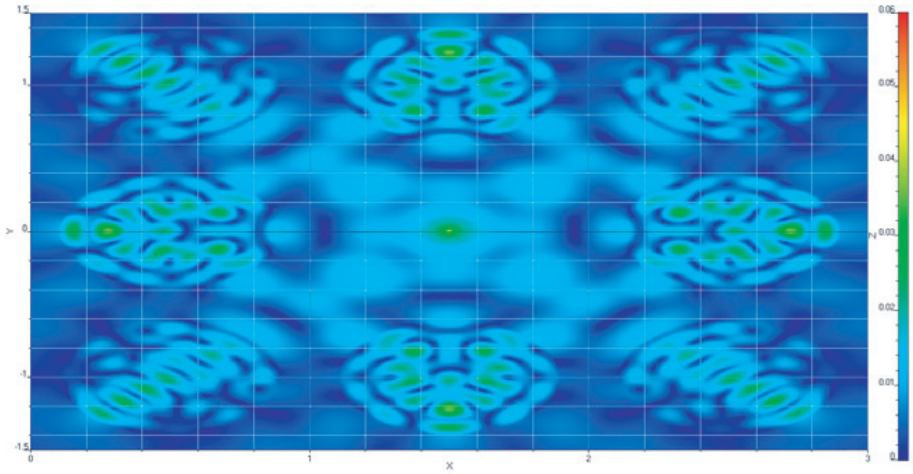

Figure 9. Magnetic field distribution of frequency = 646 THz and dielectric rods = 4.9.

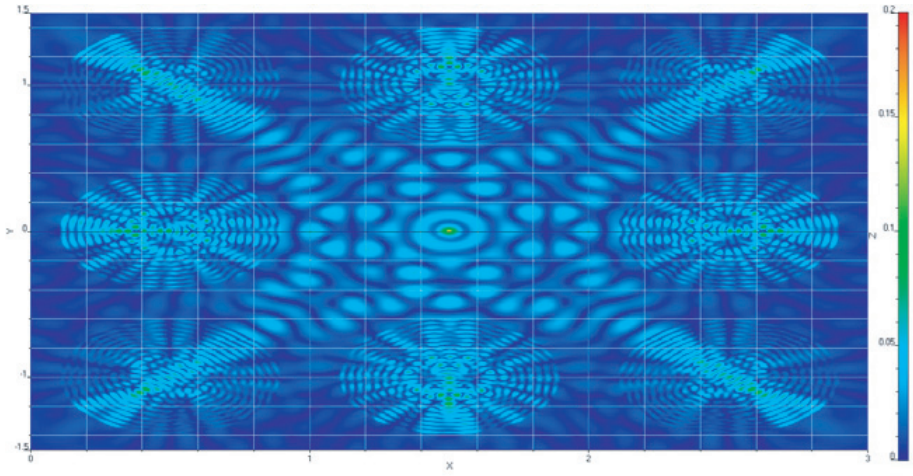

Figure 10. Magnetic field distribution of frequency = 1499 THz and dielectric rods = 12.96.

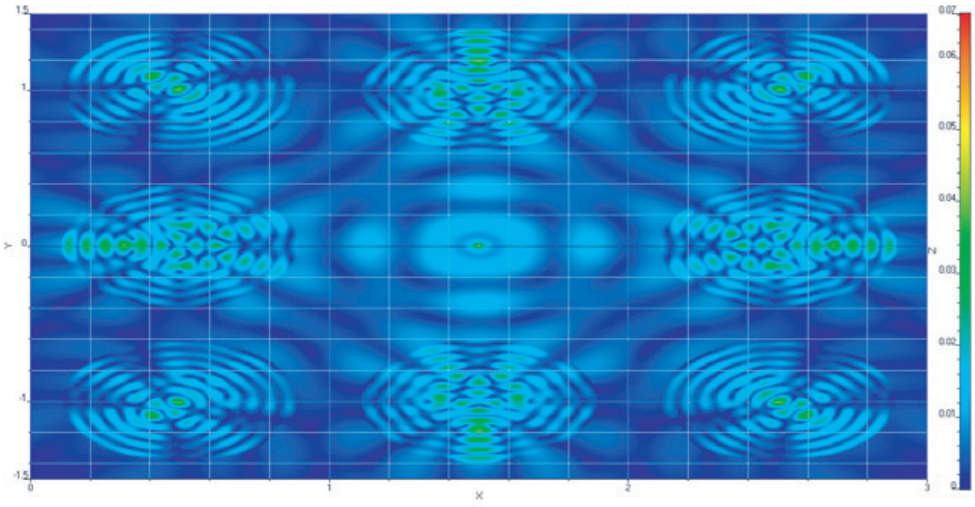

Figure 11. Magnetic field distribution of frequency = 743 THz and dielectric rods = 12.96.

4. CONCLUSION

We have plotted band structure graphs of several materials rods in a copper medium in the H polarization mode using equations derived from the literature. When the relative permittivity of the rods is increased, the effect of the surface plasmons is reduced. The characteristics of wave distribution in the structure are investigated using magnetic field distribution plots from OptiFDTD software. The plots agree very well with each other. The surface plasmon effect is detected for all the materials investigated. The surface plasmon effect is reduced when the dielectric constant of the dielectric rods is increased. Then, by using the same frequency found at band structure graph, a defect mode by removing the center rods is investigated. We find that when the dielectric constant of the rods is high, the wave is prone to propagate inside the metallic medium even lower than the plasma frequency. This phenomenon is found in different types of rods, due to the resonance state of the surface plasmon effect in the dielectric rods.

ACKNOWLEDGMENT

We would like to thank the technical staffs who participated in this project. Thanks are extended to KDU Penang University College and Universiti Sains Malaysia for the support and encouragement given.

REFERENCES

1. Yablonovitch, E., "Photonic band-gap structures," *J. Opt. Soc. Am. B*, Vol. 10, No. 2, 13, 1993.
2. John, S., "Strong localization of photons in certain disordered dielectric superlattices," *Phys. Rev. Lett.*, Vol. 58, No. 23, 4, 1987.
3. Amir Hosseini, H. N. and Yehia Massouda, "Triangular lattice plasmonic photonic band gaps in subwavelength metal-insulator-metal waveguide structures," *Appl. Phys. Lett.*, Vol. 92, 3, 2008.
4. Brand, S., R. A. Abram, and M. A. Kaliteevski, "Complex photonic band structure and effective plasma frequency of a two-dimensional array of metal rods," *Phys. Rev. B*, Vol. 75, 7, 2007.
5. Crist, A., S. G. Tikhodeev, N. A. Gippius, J. Kuhl, and H. Giessen, "Plasmon polaritons in a metallic photonic crystal slab," *Phys. Status Solidi*, Vol. 5774, No. 5, 1393–1396, 2010.
6. El-Kady, I., M. M. Sigalas, R. Biswas, K. M. Ho, and C. M. Soukoulis, "Metallic photonic crystals at optical wavelengths," *Phys. Rev. B*, Vol. 62, No. 23, 4, 2000.

7. Ghoshal, A. and P. G. Kik, "Theory and simulation of surface plasmon excitation using resonant metal nanoparticle arrays," *J. Appl. Phys.*, Vol. 103, 8, 2008.
8. Ito, T. and K. Sakoda, "Photonic bands of metallic systems. II. Features of surface plasmon polaritons," *Phys. Rev. B*, Vol. 64, 8, 2001.
9. Keskinen, M. J., P. Loschialpo, D. Forester, and J. Schelleng, "Photonic band gap structure and transmissivity of frequency-dependent metallic-dielectric systems," *J. Appl. Phys.*, Vol. 88, No. 10, 6, 2000.
10. Kuzmiak, V. and A. A. Maradudin, "Photonic band structures of one- and two-dimensional periodic systems with metallic components in the presence of dissipation," *Phys. Rev. B*, Vol. 55, No. 12, 18, 1997.
11. Kuzmiak, V. and A. A. Maradudin, "Distribution of electromagnetic field and group velocities in two-dimensional periodic systems with dissipative metallic components," *Phys. Rev. B*, Vol. 58, No. 11, 22, 1998.
12. Kuzmiak, V., A. A. Maradudin, and F. Pincemin, "Photonic band structures of two-dimensional systems containing metallic components," *Phys. Rev. B*, Vol. 50, No. 23, 10, 1994.
13. Luo, C., S. G. Johnson, J. D. Joannopoulos, and J. B. Pendry, "Negative refraction without negative index in metallic photonic crystals," *Opt. Express*, Vol. 11, No. 7, 9, 2003.
14. Moreno, E., D. Erni, and C. Hafner, "Band structure computations of metallic photonic crystals with the multiple multipole method," *Phys. Rev. B*, Vol. 65, 10, 2002.
15. O'Brien, S. and J. B. Pendry, "Photonic band-gap effects and magnetic activity in dielectric composites," *J. Physics Condens. Matter*, Vol. 14, No. 15, 11, 2002.
16. Ortuno, R., C. Garcia-Meca, F. J. Rodriguez-Fortuno, J. Marti, and A. Martinez, "Role of surface plasmon polaritons on optical transmission through double layer metallic hole arrays," *Phys. Rev. B*, Vol. 79, 10, 2009.
17. Pendry, J. B. and A. MacKinnon, "Calculation of photon dispersion relations," *Phys. Rev. Lett.*, Vol. 69, No. 19, 4, 1992.
18. Pimenov, A. and A. Loidl, "Conductivity and permittivity of two-dimensional metallic photonic crystals," *Phys. Rev. Lett.*, Vol. 96, 4, 2006.
19. Sakoda, K., N. Kawai, and T. Ito, "Photonic bands of metallic systems. I. Principle of calculation and accuracy," *Phys. Rev. B*, Vol. 64, 8, 2001.
20. Ustyantsev, M. A., L. F. Marsal, J. Ferré-Borrull, and J. Pallarès, "Effect of the dielectric background on dispersion characteristics of metallo-dielectric photonic crystals," *Opt. Commnuications*, Vol. 260, 5, 2006.
21. Xu, X., Y. Xi, D. Han, X. Liu, J. Zi, and Z. Zhu, "Effective plasma frequency in one-dimensional metallic-dieletric photonic crystals," *Appl. Phys. Lett.*, Vol. 86, 3, 2005.
22. Zeid, A. and H. Baudrand, "Electromagnetic scattering by metallic holes and its applications in microwave circuit design," *IEEE Trans. Microw. Theory Tech.*, Vol. 50, No. 4, 1198–1206, 2002.
23. Zhao, Y. and D. R. Grischkowsky, "2-D terahertz metallic photonic crystals in parallel-plate waveguides," *IEEE Trans. Microw. Theory Tech.*, Vol. 55, No. 4, 8, 2007.
24. Low, K. L., M. Z. M. Jafri, and S. A. Khan, "Effective plasma frequency for two-dimensional metallic photonic crystals," *Progress In Electromagnetics Research M*, Vol. 12, 13, 2010.
25. Low, K. L., M. Z. M. Jafri, and S. A. Khan, "Band gap calculation on 2D square lattice metallic slab photonic crystals with air rods," *3rd International Meeting on Frontiers of Physics 2009*, Kuala Lumpur, Malaysia, 2009.
26. Low, K. L., M. Z. M. Jafri, and S. A. Khan, "Band gap study using plane wave expansion method for metallic slab with air rods in E polarizing mode," *Chinese J. Phys.*, Vol. 47, No. 6, 10, 2009.
27. Low, K. L., M. Z. M. Jafri, and S. A. Khan, "Dielectric slab photonic crystals containing metallic components for E polarization mode," *Appl. Phys. Rev.*, Vol. 2, No. 2, 2010.
28. Nenninger, G. G., P. Tobiška, J. Homola, and S. S. Yee, "Long-range surface plasmons for high-resolution surface plasmon resonance sensors," *Sensors Actuators B Chem.*, Vol. 74, No. 1–3, 145–151, Apr. 2001.

29. Homola, J., S. S. Yee, and G. Gauglitz, "Surface plasmon resonance sensors: review," *Sensors Actuators B Chem.*, Vol. 54, No. 1–2, 3–15, Jan. 1999.
30. Tiwari, K., S. C. Sharma, and N. Hozhabri, "High performance surface plasmon sensors: Simulations and measurements," *J. Appl. Phys.*, Vol. 118, No. 9, 93105, Sep. 2015.
31. Homola, J., Ed., *Surface Plasmon Resonance Based Sensors*, Vol. 4, Springer Berlin Heidelberg, Berlin, Heidelberg, 2006.
32. Laude, V., Y. Achaoui, S. Benchabane, and A. Khelif, "Plane wave expansion method for phononic crystals: Review and prospects," 2009.
33. Ferre-Borrull, J., E. Xifre-Perez, M. Lluis, F. Marsal, and J. Pallares, "Real metals in metallo-dielectric photonic crystals in the visible," *2007 Spanish Conference on Electron Devices*, 4, 2007.
34. Reinhard, B., G. Torosyan, and R. Beigang, "Band structure of terahertz metallic photonic crystals with high metal filling factor," *Appl. Phys. Lett.*, Vol. 92, No. 20, 2059, 2008.
35. Zhang, J., L. Cai, W. Bai, and G. Song, "Flat surface plasmon polariton bands in Bragg grating waveguide for slow light," *J. Light. Technol.*, Vol. 28, No. 14, 2030–2036, Jul. 2010.
36. Gadot, F., A. de Lustrac, J.-M. Lourtioz, T. Brillat, A. Ammouche, and E. Akmansoy, "High-transmission defect modes in two-dimensional metallic photonic crystals," *J. Appl. Phys.*, Vol. 85, No. 12, 8499–8501, May 1999.
37. Low, K. L., M. Z. M. Jafri, and S. A. Khan, "Effective plasma frequency for two-dimensional metallic photonic crystals," *Progress In Electromagnetics Research M*, Vol. 12, No. 1, 67–79, 2010.
38. Low, K. L., M. Z. Mat Jafri, and S. A. Khan, "An investigation of surface plasmon effects on metallic photonic crystals in H polarization," *The 8th International Conference on Metamaterials, Photonic Crystals and Plasmonics*, 2017.
39. Kittel, C., *Introduction to Solid State Physics*, Wiley, 2005.
40. Sakoda, K., *Optical Properties of Photonic Crystals*, 2005.
41. Qiu, M. and S. He, "Numerical method for computing defect modes in two-dimensional photonic crystals with dielectric or metallic inclusions," *Phys. Rev. B*, Vol. 61, No. 19, 6, 2000.